Desalination and Water Treatment
www.deswater.com
doi: 10.1080/19443994.2013.792013

52 (2014) 1833–1840
February

Taylor & Francis
Taylor & Francis Group

Fabrication and characterization of microfiltration blended membranes

Sarah Farrukh*, Arshad Hussain, Nadeem Iqbal

School of Chemical & Materials Engineering, National University of Sciences & Technology (NUST), Islamabad, Pakistan
Tel. +923315447410; email: sarah@scme.nust.edu.pk

Received 18 January 2013; Accepted 24 March 2013

ABSTRACT

Woven Kevlar fabric supported polypropylene (PP)–thermoplastic polyurethane (TPU) blended microfiltration membranes were synthesized using thermally induced phase separation (TIPS) technique. Microporosity in the fabricated membranes was analyzed using scanning electron microscopy. The PP–TPU blending was confirmed through the Fourier transform infrared spectra of pure resins and blended polymer membranes. Surface roughness, pore geometry, and adhesion between the blended polymer and fabric were influenced with increasing TPU blending concentration in the PP solution. The proposed polymers were found compatible with each other and properly blended to form membranes; most importantly, the TPU helped to transform hydrophobic PP membrane into hydrophilic PP–TPU membrane. Water and methanol flux through the fabricated membranes were measured, and it was found that the permeation through the membranes depended upon the type of membrane.

Keywords: Polypropylene (PP); Thermoplastic polyurethane (TPU); Thermally induced phase separation (TIPS); Blended membrane; Hydrophobic; Hydrophilic; Contact angle

1. Introduction

The extensive use of filtration membranes has been observed from last two decades in water treatment field [1–4]. Reverse osmosis, nanofiltration, and microfiltration membranes come under this category. The pore morphology, pore distribution, and hydrophilicity of membranes and chemical resistance to feed solution are the main parameters to characterize the performance of these membranes [5,6]. The microfiltration membranes prepared using thermally induced phase separation (TIPS) technique have better fouling control characteristics compared to extruded polymeric microfiltration membranes [7,8]. A variety of polymers are used to synthesize these membranes. Recently, polyolefins are also considered as articles of trade because of their low cost and versatility [9].

Membranes can be fabricated using different techniques, such as solution casting, melt extrusion, track etching, expanded film technique, template leaching, dry–wet phase inversion technique, and TIPS. Among these, the last two methods are most commonly used. The dry–wet phase inversion technique is also called Loeb–Sourirajan technique, used by Loeb and

*Corresponding author.

Sourirajan to synthesize their first sea water desalination membrane [10]. The TIPS technique is used to fabricate polymeric membranes for microfiltration processes [7]. The phenomena behind TIPS method is that as temperature decreases, the efficiency of diluent also decreases. Sudden cooling of high temperature homogeneous solution results in the formation of two phases, one is polymer-rich phase and other is polymer-lean phase. In the end, microporous structure is formed after extraction of solvent [8,11,12].

The polypropylene (PP) is a thermoplastic and hydrophobic polyolefin. Because of exceptional pore-forming property, low cost, non–toxicity, and easy manufacturability, PP is used widely for separation and concentration; e.g. water filtration, air filtration, beverages, sea water purification, and removal of bacteria [13–15]. Several studies have been carried out to synthesize microfiltration PP membranes using TIPS technique. [16–20]. To enhance the performance of PP membranes, further chemical modifications are required. This can be achieved by surface modification (plasma treatment, irradiation with gamma rays, ion beam treatment, etc.) [21], grafting [22], and blending with different polymers.

The thermoplastic polyurethane (TPU) comes under the class of polyurethane, which is transparent, elastic, and resistant to oil, grease, and abrasion. It is used in power tools, supporting tools, medical devices, foot wear, and mobile devices [23]. Blends of TPU and Polyolefins are also reported on various aspects, such as environment, economy, and technology, which show that TPU enhances the characteristics of polyolefins [24–27].

In the present study PP is blended with different weight percentages of TPU on woven Kevlar support using TIPS technique to investigate the effect of TPU on surface morphology, pore size distribution, chemical composition, and permeation through the fabricated membranes. The blending of PP with TPU results in conversion of hydrophobic behavior of pure PP into hydrophilic behavior.

2. Materials and methods

2.1. Chemicals and reagents

PP (Guangzhou Wenlong Chemical Co.) was used as membrane-forming material. Adipic acid was used as a nucleating agent (Sigma-Aldrich). Soya bean oil was purchased from BECO (Bschawrut Enterprises Co). The TPU used in the blended membrane was received from Guangzhou Wenlong Chemical Co. Woven Kevlar fabric (K-49) was supplied by Dupont International, USA.

2.2. Experimental procedure

With different wt% concentrations of TPU, 25 wt% PP and 0.5 wt% adipic acid were immersed in the soya bean oil in separate beakers. The solution temperature was maintained at 220 °C on the magnetic stirrer for 6 h to melt and homogenize the polymers in the solution. Kevlar fabric having four inch diameter was dipped in the homogenous solution for five seconds and then quenched in the deionized water at room temperature (25 °C) for an hour. n–Hexane was used to extract the soya bean oil and then placed in the membrane in a heating oven at 80 °C to dry it. Two concentrations of TPU, i.e. 8 and 16 wt%, were blended with PP and nominated as M1 and M2, respectively.

2.3. Membrane characterization

Scanning electron microscopy (SEM, JSM 6409 A, Jeol Japan) was used to analyze the pore morphology, distribution, and geometry. Fourier transform infrared spectroscopy (FTIR) (FT-IR Spectrum 100 Perkin Elmer, mid-IR) was used to obtain the qualitative structure analysis of the blended membrane. The surface morphology/roughness of the microfiltration membranes was simulated using Scanning Probe Microscope (AFM, JSPM-5,200, Japan). X-ray diffraction machine (XRD STOE Germany Theta-Theta) was used to examine the diffraction pattern of the composite membranes. Contact angle measurements of the polymer blended membranes have been conducted using high resolution camera.

2.4. Phase diagram

To acquire phase diagrams, blended polymer–solvent–nucleating agent samples with various polymer blended concentration were synthesized as described in Section 2.2. After drying, a little amount of sample was loaded in capillary tubes, which were purged with nitrogen gas to avoid oxidation reaction. These capillary tubes were heated at 493 K in electrothermal apparatus (Merck 9100). The samples were completely melted immediately. These samples were cooled at 10 K/min. The cloud point was observed when turbidity appeared in samples through optical eye glasses, which were attached with electrothermal equipment.

2.5. Permeation study

The prepared membranes, M1 and M2, were put into permeation test to analyze the pure water and

methanol flux through them. For this, a domestically manufactured filtration cell with 1L capacity and base circular area of 13.84 cm^2 at feed pressure of 0.1 MPa was used. The flux, J (L/m^2h), through the membranes was measured using Eq. (1) as follows:

$$J = V/At \quad (1)$$

where V is the volume of solvent permeated, A is the effective membrane area, and t is the permeation time.

3. Results and discussions

3.1. Phase diagram

Generally, in TIPS, diluent is used to dissolve polymer with heating. As the temperature of polymer–diluent mixture lowers, liquid–liquid demixing starts and generates two phases, polymer rich and polymer lean. Polymer-lean phase mainly consists of diluent and creates voids after extraction with a particular solvent. Polymer-rich phase develops membrane's structure. Fig. 1 represents the phase diagram of blended polymer–solvent–nucleating agent. The upper critical solution temperature for liquid–liquid phase separation was observed. Above 0.2 weight fraction of blended polymer, the T_{cloud} (cloud temperature) decreases with increasing concentration of blended polymer, keeping the concentration of nucleating agent constant. At 0.1 weight fraction of blended polymer, the T_{cloud} was observed at a value lower than 0.2 weight fraction-blended polymer. This can be caused by small concentration difference between polymer-rich and polymer-lean phases. The refractive index difference of both phases is very small and cannot be easily visualized, whereas at high blended polymer concentration, polymer-rich phase and polymer-lean phase have high concentration difference so that liquid–liquid demixing can easily be observed with optical eye glasses [28–30]. The observed curve shows binodal, as the region above the curve is homogeneous region, whereas the portion below this curve elaborates the polymer–diluent demixing region.

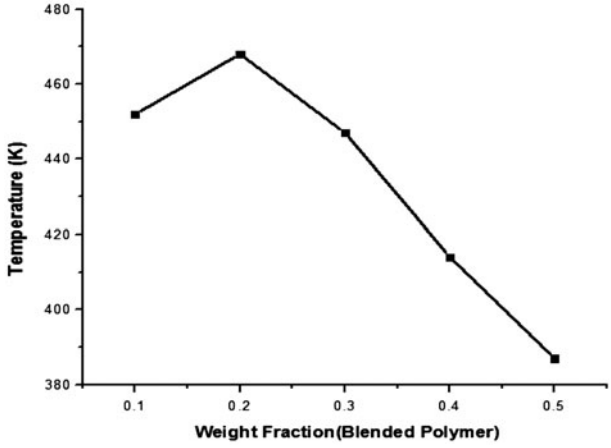

Fig. 1. Phase diagram of blended polymer–solvent–nucleating agent.

3.2. SEM analysis

In SEM micrographs in Fig. 2(a,b), two different magnifications confirm the microporosity generation in the polymer-blended composite membrane (M1). Uniform and homogeneous pores have been developed throughout the membrane. The pore geometry is not aptly circular and pore diameter range is 0.1–3 μm.

SEM micrographs of M2 composite membranes are depicted in Fig. 3(a,b). TIPS technique has successfully generated uniformly distributed porosity in the polymer-blended membrane. The pore size range of M2 membrane is 75.66 nm–3 μm. Appropriately, all pores have circular geometry throughout the membrane. TPU-blending concentration has remarkably affected the pore morphology/size of the composite membrane.

The SEM micrographs of the cross section of the composite membranes are elucidated in Fig. 4. The membrane cross-sectional measurements revealed that the polymeric film and total thicknesses of the synthesized membranes were augmented with increasing the TPU-blending concentration in the PP solution. The total thickness of M1 and M2 micro membranes were found to be 0.66 and 0.76 mm, respectively. The one-side thicknesses of the blended polymeric film on the Kevlar substrate were measured as 0.22 and 0.27 mm for the M1 and M2 membranes, respectively. The presented images demonstrate that porous structure is also developed within the membranes' cross section, using TIPS technique.

3.3. AFM analysis

AFM is a well-known technique to study the surface roughness and morphology of membranes. AFM images of the blended membranes are given in Fig. 5 (a,b). The surface of M1 membrane is little bit wavy and nearly smooth. The average roughness is 11.4 nm and root mean square value is 14.1 nm. The maximum height of the M1 membrane is 92.1 nm, whhich adhered on the Kevlar facet. On the other hand, the overall roughness of M2 membrane is 45.2 nm, which is quite high compared to the M1 membrane. Root mean square value for M2 membrane is 58.4 nm and the maximum height is 405.5 nm.

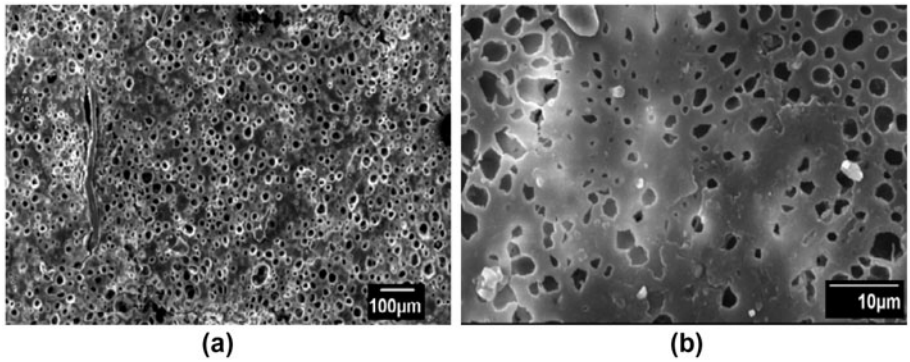

Fig. 2. SEM micrographs of PP–TPU (M1) membrane at different magnifications.

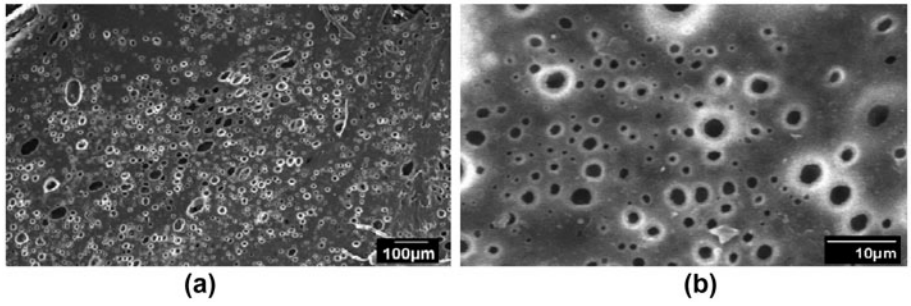

Fig. 3. SEM micrographs of PP–TPU (M2) membranes at different magnifications.

Fig. 6 represents the AFM images of the fabricated membranes with larger scan area (100 μm^2). These images clearly indicates that with increasing TPU concentration in PP solution, the surface roughness of the membrane is augmented, which endorses the SEM findings.

3.4. FTIR spectrum analysis

Functional group analysis of membranes is generally explored by FTIR. Fig. 7 represents FTIR spectrum of the fabricated membranes. The FTIR spectra of pure PP and TPU are already reported in the literature [31,32].

The combination of PP and TPU in blended membranes are confirmed by CH peak at 2,858 cm^{-1}; strong bands near 1,455 and 1,376 cm^{-1} represent bending transmittance of CH_2 and CH_3 groups (assigned as PP skeleton feature) and NH peaks at 3431 cm^{-1} (stretching) and 1,634 cm^{-1} (bending) in M1 membrane and 3,438 cm^{-1} (stretching) and 1646 cm^{-1} (bending) in M2 membrane (specific for TPU). The effect of increasing concentration of TPU in blending results in diminishing of peak at 2,858 cm^{-1} that is distinctive for PP. Another visible change of increasing TPU concentration is the appearance of isocayanate functional group –N==C==O peak at 2321 cm^{-1} that is also a typical feature of TPU. The M1 peaks are sharp and distinguishable, but with increasing TPU concentration peaks are getting broad. The FTIR spectra of pure PP and TPU are also presented in Fig. 7. The acquired data revealed that the major spectrum peaks found for pure polymers were in league with the M1 and M2 transmittance peaks.

3.4. XRD analysis

The XRD spectra of pure TPU and PP are explained in different research papers. According to literature, five peaks at $2\theta = 14.19°$, $16.98°$, $18.63°$, $25.72°$, and $28.35°$ are observed in the diffraction pattern of pure PP [31]. Whereas for pure TPU, broad diffraction peak with maximum intensity are appeared at around $2\theta = 19.75°$ [32]. It is clear from Fig. 8 that all peaks of pure PP and TPU are present in XRD spectra of M1 and M2 membranes. Therefore, blending of PP and TPU is assured by this result. However, the peak for TPU in M1 blend is not much prominent as in M2 blend due to low concentration of TPU in aforementioned case. Another obvious change is that all peaks are sharp, compared with pure PP and TPU. This can be a possible effect of blending.

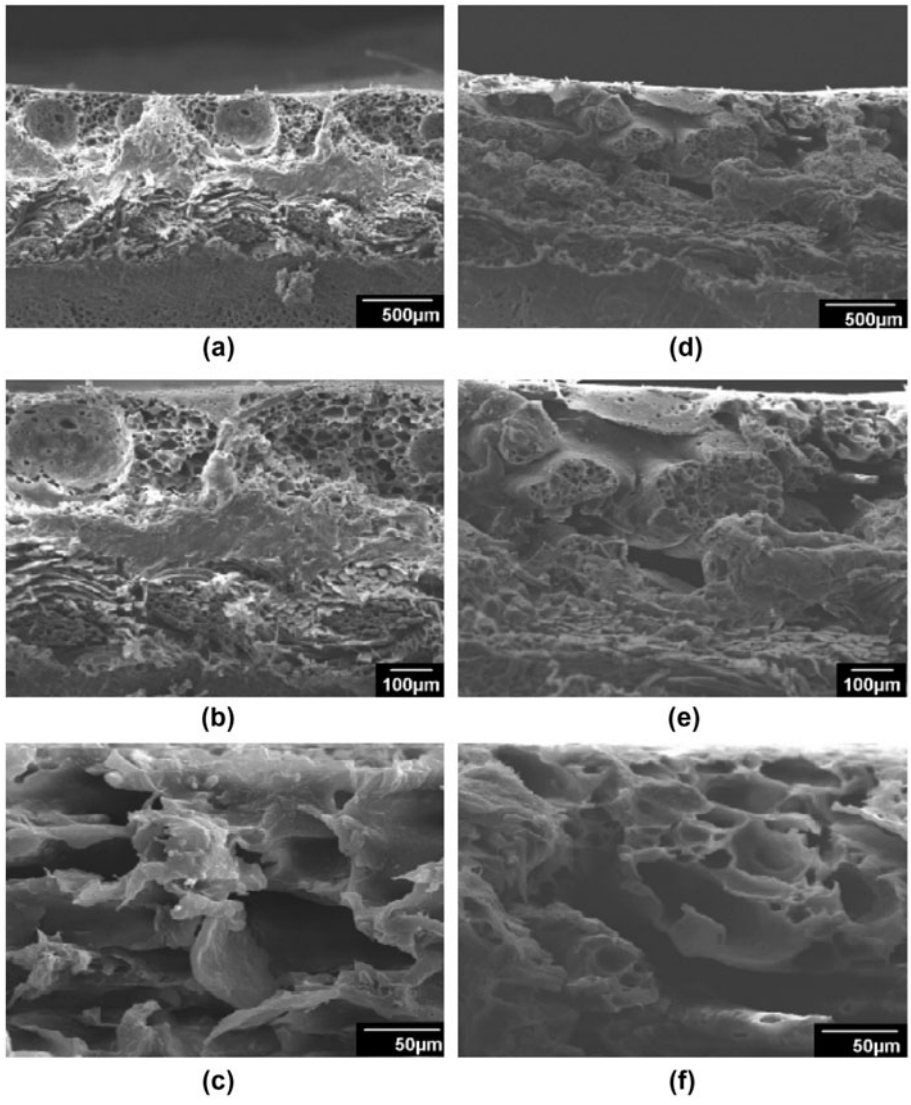

Fig. 4. Cross-section images of M1 (a,b,c) and M2 (d,e,f) membranes.

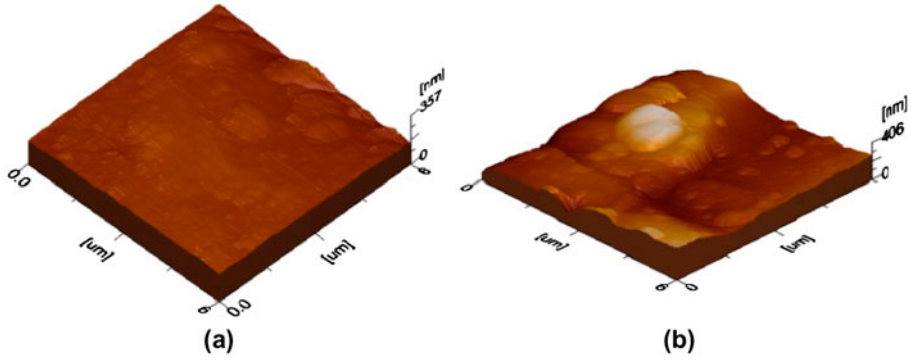

Fig. 5. The surface morphology of M1 (a) and M2 (b) membranes, respectively, at scan area of 36 μm^2.

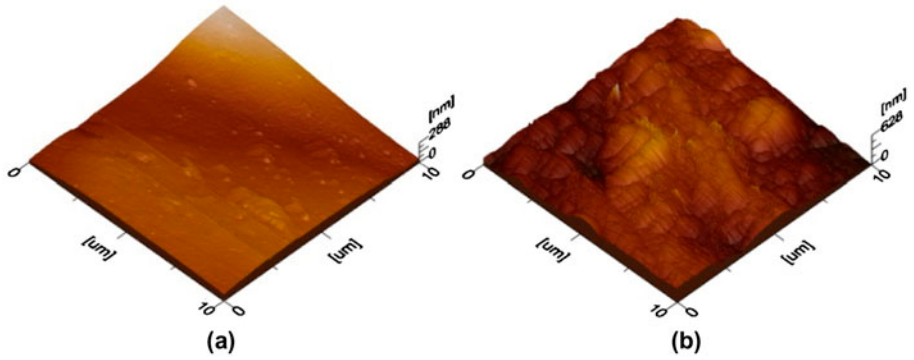

Fig. 6. The surface morphology of M1 (a) and M2 (b) membranes, respectively, at the scan area of 100μm^2.

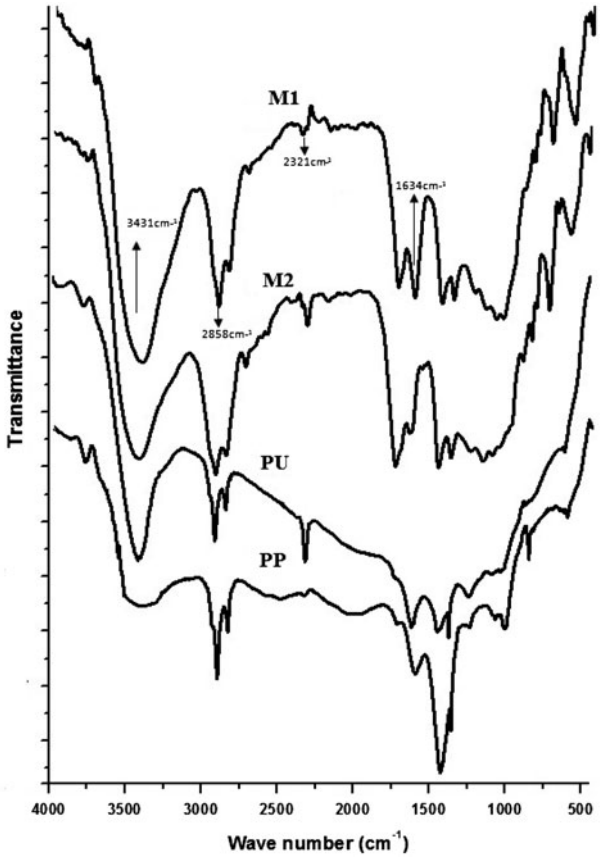

Fig. 7. FTIR spectra of PP, TPU, M1, and M2 membranes.

The major peaks found in the XRD patterns of the pure PP and TPU were similar to that of M1 and M2 composite membranes' diffraction peaks.

3.5. Contact angle measurement

Contact angle measurement is a criterion to investigate the wettability of membranes. Membranes can be grouped into three categories, i.e. hydrophobic,

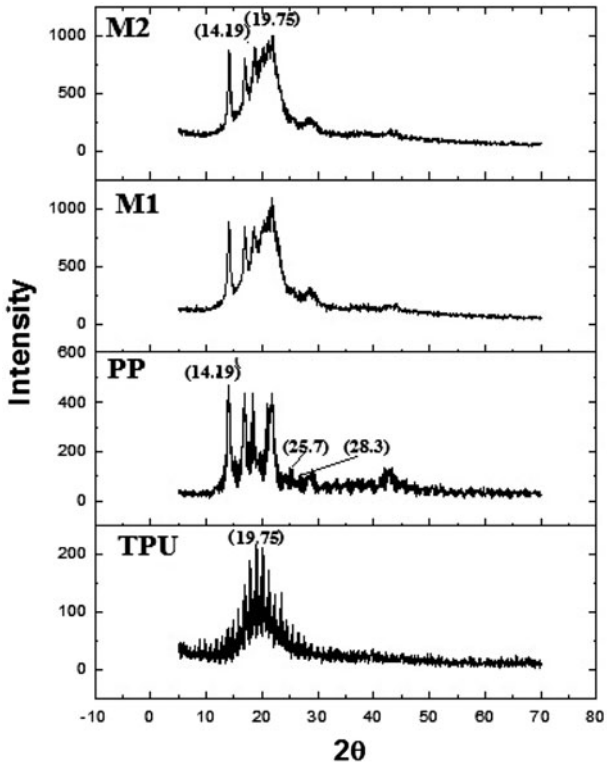

Fig. 8. XRD spectrum of pure and blended membranes.

hydrphilic, and penetrating, depending on the (θ) value. Membranes with θ values equal to 110° are classified as hydrophobic membranes, whereas hydrophilic membranes have (θ) value near to 70°. However, in penetrating membranes θ has approximately 0° value [33]. The contact angle actually quantifies the magnitude of cohesive and adhesive forces between liquid and solid surface. The cohesive forces of liquid are weaker than adhesive forces in hydrophilic membranes and stronger in hydrophobic membranes. These values are dependent on porosity, surface roughness, and chemical compositions of membranes under study [34,35]. Comparison of

wetting characteristics of blended membranes with pure PP was made by the contact angle measurements of the fabricated composite membranes, and the acquired data are presented in Table 1.

It is obvious from Table 1 that the contact angle of M1 and M2 membranes is diminished with the incorporation of TPU in the PP solution. The 8 and 16wt% blending of TPU with PP reduce the contact angle to 20.5 and 30.5°, respectively, compared to the pristine PP membrane (85.5°). It illustrates that the TPU incorporation into the PP solution has successfully transformed the nature of the fabricated membrane, from hydrophobic to hydrophilic. Pure PP lacks polar groups for chemical attachment with substrate (Kevlar). Chemical modifications are required to increase polar groups in PP. In general, the treatment of hydrophobic membranes is carried out with a hydrophilic polymer that improves the membrane wettability [36]. In accordance with this fact, the blending of hydrophilic TPU enhances the wettability of pure PP. As TPU has N–H and –N==C==O functional groups, they develop strong linkage between the adhesive and the adherent. Also, it improves the interfacial strength between the fabric and the blended polymer that results in lowering of the contact angle of the fabricated membranes [33,37,38]. Lower contact angle values of blended membranes make them more hydrophilic and not vulnerable to organic compounds, as compared to pure PP membranes. Another distinguishing property of hydrophilic membrane is its roughness; more the roughness, less will be the contact angle. So, blended membranes acquire more roughness with increasing concentration of TPU and it is also supported by AFM results explained already.

3.6. Membrane performance

The permeation efficiency of M1 and M2 membranes were examined by measuring pure water and methanol flux through these membranes, and the obtained data are presented in Fig. 9. The solvent flux through the membrane is higher for the composite membrane prepared with high concentration of TPU compared to the rest one due to the pore size and hydrophilicity enhancement with increasing the TPU contents in the membrane solution. These findings are also supported by SEM and AFM results (Figs. 2–6). In addition, water flux through the membranes was observed higher compared to methanol owing to the small water molecule size (0.26 nm), in contrast with methanol (0.41 nm).

Table 1
Contact angles of pure PP and blended membranes (M1 & M2) to illustrate wetting characteristics

Material	Θ	Cos θ	Wetting characteristic
Pure PP [33]	84°	0.1045	Hydrophobic
Pure PP	85.5°	0.7794	Hydrophobic
M1 membrane	65°	0.4226	Hydrophilic
M2 membrane	55°	0.5735	Hydrophilic

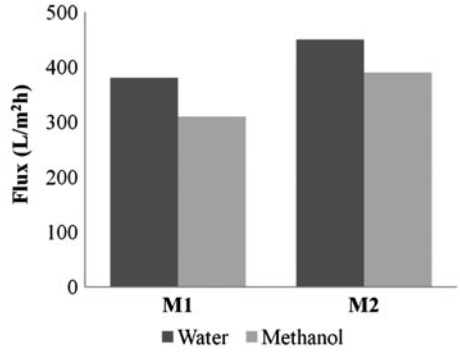

Fig. 9. Water and methanol flux through M1 and M2 membranes.

4. Conclusions

In this study, TIPS technique is implied to fabricate PP–TPU blended membranes, in which Kevlar fabric is used as a membrane support. The effect of TPU-blending concentration on the pore morphology, pore distribution, average pore size, and hydrophobicity of the pure PP membrane is scrutinized. The blended membranes are characterized using SEM, AFM, FTIR, XRD, micro-filtration assembly, and contact angle measurement. SEM micrographs illustrate that pore morphology and size are influenced with increasing TPU concentration in the membrane solution. FTIR and XRD study confirm the presence of proposed polymers in the blended membranes. The AFM images elaborate the roughness and film thickness enhancement with increasing TPU concentration. The contact angle measurement of the fabricated membranes illustrates the augmentation of hydrophilic nature of the pristine PP membrane with increasing TPU contents in the PP solution. The flux study reveals that with increasing the TPU concentration in the membrane solution, permeation through the fabricated membrane is enhanced accordingly.

References

[1] B. Tansel, J. Regula, R. Shalewitz, Treatment of fuel oil and crude oil contaminated waters by ultrafiltration membranes, Desalination 102 (1995) 301–311.
[2] Y.H. Wan, X.D. Wang, X.J. Zhang, Treatment of high concentration phenolic waste water by liquid membrane with N503 as mobile carrier, J. Membr. Sci. 135 (1997) 263–270.

[3] S. Mondal, S.R. Wickramasinghe, Produced water treatment by nanofiltration and reverse osmosis membranes, J. Membr. Sci. 322 (2008) 162–170.
[4] C.O. M'Bareck, Q.T. Nguyen, S. Alexandre, I. Zimmerlin, Fabrication of ion-exchange ultrafiltration membranes for water treatment: I. Semi-interpenetrating polymer networks of polysulfone and poly(acrylic acid), J. Membr. Sci. 278 (2006) 10–18.
[5] J. Wang, W. Ruan, J. Ji, K. Yao, Dead-end filtration properties of microporous polypropylene membranes with different gas permeation rates, Desalination 192 (2006) 68–73.
[6] R. Mülhaupt, Catalytic polymerization and post polymerization catalysis fifty years after the discovery of Ziegler's catalysts, Macromol, Chem. Phys. 204 (2003) 289.
[7] M.E. Vanegas, R. Quijada, D. Serafini, Microporous membranes prepared via thermally induced phase separation from metallocenic syndiotactic polypropylenes, Polymer 50 (2009) 2081–2086.
[8] S.W. Song, J.M. Torkelson, Coarsening effects on microstructure formation in Isopycnic polymer solutions and membranes produced via thermally induced phase separation, Macromolecules 27 (1994) 6389–6397.
[9] S.S. Rincón, Nuevos desarrollos en PP: Copolímeros heterofásicos de alto módulo, Revista Plásticos Modernos 83 (2002) 307.
[10] R.W. Baker, Membranes Technology and Its Applications, second edition, Wily, West Sussex, 2004.
[11] P.M. Atkinson, D.R. Lloyd, Anisotropic flat sheet membrane formation via TIPS: Thermal effects, J. Membr. Sci. 171 (2000) 1–18.
[12] S.S. Kim, D.R. Lloyd, Microporous membrane formation via thermally-induced phase separation. III. Effect of thermodynamic interactions on the structure of isotactic polypropylene membranes, J. Membr. Sci. 64 (1991) 13–29.
[13] T. Shimokawa, M. Shoda, Y. Sugano, Purification and characterization of two DyP Isozymes from Thanatephorus Cucumeris Dec 1 specifically expressed in an air-membrane surface bioreactor, J. Biosci. Bioeng. 107 (2009) 113–115.
[14] B. Veleirinho, F.A. Lopes-da-Silva, Application of electro spun Poly (ethylene terephthalate) nanofiber mat to apple juice clarification, Process Biochem. 44 (2009) 353–356.
[15] C. Charcosset, Preparation of emulsions and particles by membrane emulsification for the food processing industry, Food Eng. 92 (2009) 241–249.
[16] A.J. Castro, US Pat. No. 4,247,498 (1981).
[17] D.R. Lloyd, S.S. Kim and K.E. Kinzer, Microporous membrane formation via thermally induced phases separation. II. Liquid–liquid phase separation, J. Membr. Sci. 64 (1991) 1.
[18] W. Yave, R. Quijada, D. Serafini, D.R. Lloyd, Effect of the polypropylene type on polymer–diluent phase diagrams and membrane structure in membranes formed via the TIPS process: Part I. Metallocene and Ziegler–Natta polypropylenes, J. Membr. Sci. 263 (2005) 146–153.
[19] C.D. Rosa, F. Auriemma, R. Mulhaupt, Structure and physical properties of syndiotactic polypropylene: A highly crystalline thermoplastic elastomer, Polymer 37 (1996) 2627–2634.
[20] M.E. Vanegas, R. Quijada, D.serafini, Microporous membranes prepared via thermally induced phase separation from metallocenic syndiotactic polypropylenes, Polymer 50 (2009) 2081–2086.
[21] Y. Wang, J. Kim, K. Choo, Y. Lee, C. Lee, Ozone-induced graft polymerization onto polymer surface, J. Membr. Sci. 169 (2000) 269–276.
[22] Q. Yang, Z.K. Xu et al., Surface modification of polypropylene microporous membranes with a novel Glycopolymer, Chem. Mater. 17 (2005) 3050–3058.
[23] Y. Hamid, B. Mehdi, N.K. Feriedoun, Synthesis and properties of novel thermoplastic poly (urethane-imide)s, Eur. Polym. J. 36 (2000) 2207–2211.
[24] Q.W. Lu, C.W. Macosko, Comparing the compatibility of various functionalized polypropylenes with thermoplastic polyurethane (TPU), Polymer 45 (2004) 1981–1991.
[25] T. Tang, X. Jing, B. Huang, Studies on compatibilization of polypropylene/thermoplastic polyurethane blends and mechanism of compatibilization, J. Macromol. Sci.-Phy. B. 33 (2006) 287–305.
[26] K. Wallheinke, P. Pötschke, H. Stutz, Influence of compatibilizer addition on particle size and coalescence in TPU/PP blends, J. Appl. Polym. Sci. 65 (1997) 2217–2226.
[27] K. Wallheinke, P. Pötschke, C.W. Macosko, H. Stutz, Coalescence in blends of thermoplastic polyurethane with polyolefins, Polym. Eng. Sci. 39 (2004) 1022–1034.
[28] Y.R. Qiu, H. Matsuyama, Preparation and characterization of poly(vinyl butyral) hollow fiber membrane via thermally induced phase separation with diluent polyethylene glycol 200, Desalination 257 (2010) 117–123.
[29] H. Matsuyama, M. Teramoto, M. Kuwana, Y. Kitamura, Formation of polypropylene particles via thermally induced phase separation, Polymer 41 (2000) 8673–8679.
[30] W. Yave, R. Quijada, M. Ulbricht, R. Benavente, Syndiotactic polypropylene as potential material for the preparation of porous membranes via thermally induced phase separation (TIPS) process, Polymer 46 (2005) 11582–11590.
[31] L. Singh, R. Singh, Swift heavy ion induced modifications in polypropylene, Nucl. Instrum. Methods Phys. Res. B. 225 (2004) 478–482.
[32] A.K. Barick, D.K. Tripathy, Effect of nanofiber on material properties of vapor-grown carbon nanofiber reinforced thermoplastic polyurethane (TPU/CNF) nanocomposites prepared by melt compounding, Compos. A. 41 (2010) 1471–1482.
[33] C.O. Putman, U.K. Vaidya, Mechanisms of interfacial adhesion in metal–polymer composites—effect of chemical treatment, Compos. A. 42 (2011) 906–915.
[34] M. Olteanu, D. Achimescu, Z. Vuluga, V. Trandafir, Measurement and interpretation of wetting properties of new collagen-silicate biomaterial, Revue Roumaine de Chimie 53 (2008) 157–163.
[35] S. Raghav, Polymer filled nanoporous membranes, M.S. Thesis, Drexel University, USA, 2005.
[36] S.X. Liu, J.T. Kim, S. Kim, Effect of polymer surface modification on polymer–protein interaction via hydrophilic polymer grafting, JFS E: Food Eng. Phys. Prop. 73 (2008) 143–150.
[37] S.K.N. Kutty, G.B. Nando, Self adhesion of short Kevlar fibre-thermoplastic polyurethane composite, J. Adhes. Sci. Technol. 7 (1993) 105–113.
[38] S.K. De, J.R. White, Short Fibre: Polymer Composites, first edition. Woodhead, 1996.